

Mesh adaptation by Optimal Control of a continuous model

François Courty, Tristan Roy, Bruno Koobus, Alain Dervieux

► **To cite this version:**

| François Courty, Tristan Roy, Bruno Koobus, Alain Dervieux. Mesh adaptation by Optimal Control of a continuous model. [Research Report] RR-5585, INRIA. 2006, pp.31. inria-00070422

HAL Id: inria-00070422

<https://hal.inria.fr/inria-00070422>

Submitted on 19 May 2006

HAL is a multi-disciplinary open access archive for the deposit and dissemination of scientific research documents, whether they are published or not. The documents may come from teaching and research institutions in France or abroad, or from public or private research centers.

L'archive ouverte pluridisciplinaire **HAL**, est destinée au dépôt et à la diffusion de documents scientifiques de niveau recherche, publiés ou non, émanant des établissements d'enseignement et de recherche français ou étrangers, des laboratoires publics ou privés.

Mesh adaptation by Optimal Control of a continuous model

F. Courty, T. Roy, B. Koobus, A. Dervieux

N° 5585

May 13, 2005

Thème NUM



*Rapport
de recherche*

Mesh adaptation by Optimal Control of a continuous model

F. Courty*, T. Roy†, B. Koobus‡, A. Dervieux§

Thème NUM — Systèmes numériques
Projet Tropics

Rapport de recherche n° 5585 — May 13, 2005 — 31 pages

Abstract: The problem of finding the best mesh in a numerical simulation is addressed with the introduction of a scalar output and of an adjoint state in combination with an *a priori* error model. This strategy is organised around a continuous modelling of mesh description and numerical error. The mesh description is done by the specification of a continuous metric([7]). This is a scalar field defining the mesh fineness over the domain. A truncation error is modelled from an *a priori* estimate in function of the metric. The numerical error is then derived from the truncation error using a "state system" having the truncation error as right hand side. This allows to formulate the optimal mesh problem under the form of a continuous Optimal Control problem, with a control, the metric, a state equation, the error equation, and a functional, the error on scalar output. The minimisation with respect to the metric is applied under a control constraint expressing the fact that the equivalent mesh has a specified number of nodes. Examples dealing with elliptic model problems will be presented. The optimisation process is implemented with a gradient method and produce the optimal metric. Then an adapted mesh is generated. This process is reiterated a few times.

Key-words: Partial Differential Equations, Finite Elements, mesh adaptation, adjoint state, error estimates, optimisation

* INRIA, 2004 Route des Lucioles, BP. 93, 06902 Sophia-Antipolis, France

† INRIA, 2004 Route des Lucioles, BP. 93, 06902 Sophia-Antipolis, France

‡ Université de Montpellier II, Place Eugène Bataillon, Département de Mathématiques, CC 051, F-34095 Montpellier Cedex 5 and INRIA

§ INRIA, 2004 Route des Lucioles, BP. 93, 06902 Sophia-Antipolis, France

Adaptation de maillage par le contrôle optimal d'un modèle continu

Résumé : Afin de profiter d'avancées théoriques sur la convergence des techniques de maillages adaptatifs, telles que [10],[7], on formule le problème de l'optimisation du maillage en fonction d'un critère à minimiser vis-à-vis d'un paramétrage continu du maillage, la "métrique continue". Ce champ décrit le raffinement local du maillage. Pour le prendre en compte dans notre formulation, il faut modéliser l'erreur d'approximation de l'équation aux Dérivées Partielles elliptique considérée en fonction de la métrique continue. Divers aspect de cette approche sont analysés.

Mots-clés : Equations aux Dérivées Partielles, Eléments Finis, Adaptation de maillage, état adjoint, estimations d'erreur, optimisation

Contents

| | | |
|----------|--|-----------|
| 1 | Introduction | 2 |
| 2 | A finite-difference based model | 4 |
| 2.1 | Simplifying assumptions for truncation error | 4 |
| 2.2 | Mesh adaptation problem formulation | 4 |
| 2.3 | A paradox | 5 |
| 2.4 | Regularized optimisation problem | 6 |
| 2.5 | Optimality conditions | 8 |
| 3 | A finite-element based continuous model | 9 |
| 3.1 | Implicit error | 9 |
| 3.2 | Truncation error analysis | 11 |
| 3.3 | Implicit error model | 12 |
| 4 | Optimal Control model | 14 |
| 5 | Numerical experiments | 15 |
| 5.1 | Adaptative mesh algorithm | 15 |
| 5.2 | Numerical experiments: Finite Differences | 16 |
| 6 | Conclusions | 19 |
| 7 | Appendix: Estimates for truncation term | 21 |
| 7.1 | Assumptions on mesh regularity | 21 |
| 7.2 | Study of A_1 | 23 |
| 7.3 | Analysis of term A_2 | 26 |
| 7.4 | Determination of main term of A'_1 | 29 |

1 Introduction

Mesh adaptation is a challenging question in which performances of the different techniques can be theoretically analysed. A central question is the numerical order of convergence, which can be improved by mesh adaptation [7],[10]. The problem of finding the best mesh in a numerical simulation is progressively receiving answers with the introduction of a scalar output and of an adjoint state in combination with *a posteriori* estimates (see for example [3]). In the present work, the proposed strategy is organised around a continuous modelling of mesh description and *a priori* numerical error. An important difficulty in mesh adaptation is the choice of the quantities that will prescribe the fineness of the adapted mesh. Indeed, the approximation error is a complex non-local function of mesh fineness. The main idea to solve this difficulty is to identify the error as the solution of a continuous or discrete linear error system with a right hand side, the truncation error that should depend only on the local quality of the mesh. Two families of mesh adaptation methods can be distinguished. In a first set of works, a particular function of the dependant variable, the **sensor**, is chosen and its derivatives are considered as a good local truncation error indicator. This can be justified in the case of Hessian based adaptation (see for example [4],[9],[1]). Indeed, the proposed indicator is derived from interpolation error, and, in the case of finite-element approximations, a classical *a priori* error analysis shows that approximation error is smaller than the interpolation error. The paramount interest of this approach for anisotropic adaptation is a very sound indication of the necessary stretching of the mesh. Another important feature is that it involves the research of an ideal mesh.

In a second series of works, several authors propose a rather accurate definition of the purpose of the adaptation. It is to minimize a norm of the error or a real-valued functional to compute accurately. Then adjoint-based *a posteriori* error estimates were systematically derived from this specification. This allowed to compute an error level and to refine the regions where the local truncation error is larger than a tolerance ([3],[11]). The fact that effective *a posteriori* errors are controlled is an advantage of this kind of methods. These works are progressing towards anisotropic adaptation. One difficulty on this way is that corrections with respect to an existing mesh are managed instead of the specification of an ideal mesh which should not depend on the current mesh.

The first approach has been explored for finding the best mesh interpolating a given analytic function. This optimal mesh standpoint was described as the “mesh optimality method” in Chap.3 of [2]. The “continuous metrics method” was elaborated in [7] for that simpler problem. The ideal mesh to be found is defined by a continuous scalar fields, typically one single mesh node density for describing an ideal isotropic mesh (i.e. without stretching), or a diagonalisable positive matrix for describing an ideal anisotropic mesh (with a control of the local stretching). An important point concerns the *mesh size*: the ideal mesh is normalized in such a way that we can answer to any prescription of the total number N of nodes by defining the local density as the product of the normalized one by N .

Two important consequences of this option concern (1) mesh quality and (2) superconvergence.

Mesh quality issues arise when a mesh generation tool is applied to get a rough compromise

between mesh quality and mesh size. If we describe with a single function a family of meshes some of which can be arbitrarily fine, we can theoretically build them with a perfect quality (e.g. smoothness and good angles). As a consequence, the proposed method assumes that for any ideal metric, for any “large enough” number of nodes, a mesh with perfect quality will be build from it. Mesh quality is thus neither modelled nor taken into account in the proposed method.

Superconvergence: In a first phase of the developement of the continuous metric method, the model chosen for the local error will be simplified to a single term. This term is then of a particular order α with respect to mesh size. To be coherent with the mesh quality assumption, superconvergence error estimate are favourized (second order for linear finite-elements).

Going further in this discussion, we conclude that we should not take into account in our *a priori* error analysis the singular components of the approximation error that are carried by the inter-element singularities of the finite-element interpolation. In other words, we shall restrict to component of the error that is *smooth and independant of mesh tessellation location*.

The extension of the continuous metric method to Partial Differential Equation mesh adaptation takes some inspiration from adjoint-based error estimates. But it goes a little further in the direction of setting the mesh adaptation problem as a standard optimal control problem.

The extension proposed here will focus on an elliptic partial differential equation.

After examining on a simplified model some difficulties which may arise from formulations dedicated to the approximation error minimisation, we shall propose a finite-element model for the PDE extension of the continuous metric method. Then some numerical experiments are presented.

2 A finite-difference based model

Even when the number of nodes is fixed, the minimisation of the approximation error with respect to mesh density is not always a well posed problem. We first discuss this point in a simplified context.

2.1 Simplifying assumptions for truncation error

The local truncation error is highly dependent of the local regularity of the mesh, for example, from the variation of mesh step in one direction, from the number of neighbors of a given node, from the regularity of the triangles.

In the case of an *a posteriori* error estimate, it is natural to try to get an exact information about the error size due to the different characteristics of the current mesh.

Conversely, we can try to specify a mesh that is as good as possible for a given purpose. This means that:

- the mesh is adapted to the purpose,
- the mesh is of high quality, i.e. both topology and metric properties (smoothness of local mesh size and stretching) are regular.

In our standpoint, we admit that if we can produce a regular enough continuous metric that answers to the first criterion, adaptation to the purpose, then the application of a good mesh generator, controlled by the metric, will produce meshes that satisfy both criteria.

To fix the ideas, the following local smoothness assumptions are made for the adapted mesh:

- a molecule around a node is close to a symmetric regular one,
- in the case of isotropy, the molecule is regularly put on a circle,
- in the case of anisotropy, we restrict to the scalar case and the previous molecule is regularly put on an ellipse, whose main axes are aligned with the Hessian of the PDE solution to compute.

Remark: In the case of singularities, the error estimate will not be directly valid as such but rather as a singularity indicator.

2.2 Mesh adaptation problem formulation

We start first with a finite-difference model. In the isotropic case, and for the case of Laplace equation we shall use the cartesian finite difference approximation on five points. Transposed formally to the continuous context, the model for truncation error gives:

$$T_{te}(u, x, y) = h(x, y)^2 |u^{(4)}|(x, y) \quad (1)$$

where $|u^{(4)}|(x)$ holds for the largest modulus of the four eigenvalues of the fourth derivative matrix of u .

$h(x, y)$ is the local mesh size, the length of discretisation step in any direction.

We write in short:

$$T(u, x, y) = h^2 m(u) ; m(u) \text{ a function of } u .$$

The mesh density, i.e. the local number of nodes in a unit volume is:

$$d(x, y) = h(x, y)^{-2} .$$

The problem of the best accuracy can be described by the following continuous formulation:

$$\text{Find } d = \text{Argmin } |\mathcal{A}^{-1} d^{-1} m(u)|_{L^2}^2$$

where \mathcal{A} denotes the isomorphism between H_0^1 and H^{-1} :

$$v = \mathcal{A}^{-1} f \Leftrightarrow f = \mathcal{A}v \Leftrightarrow -\Delta v = f \text{ in } \Omega, v|_{\partial\Omega} = 0 ,$$

with the constraint of a given number N of nodes, which writes:

$$\int d = N .$$

Remark: In (1), we have chosen a second-order leading term and have neglected higher-order errors. When this term vanishes, this model tends to indicate that error is vanishing while, instead, the error is asymptotically of higher order.

Remark: In (1), we have also replaced a function by its absolute value. This means that we get an upper bound for truncation error. If this truncation error bound is used as the right-hand side of an approximation error equation, we shall obtain an approximation error bound if the operator has adhoc positivity or monotonicity properties. In the present case we enjoy a maximum principle.

2.3 A paradox

The minimisation problem can be written as :

$$\begin{aligned} \text{Find } d = \text{Argmin } |\mathcal{A}^{-1} d^{-1} m(u)|_{L^2}^2 \\ \text{under the constraint } \int d = N \end{aligned} \tag{2}$$

Let $\bar{d} = d/N$. We get:

$$\begin{aligned} \text{Find } \bar{d} = \text{Argmin } N^{-2} |\mathcal{A}^{-1} \bar{d}^{-1} m(u)|_{L^2}^2 \\ \text{under the constraint } \int \bar{d} = 1 \end{aligned} \quad (3)$$

When \bar{d} is the optimum, the optimality condition of this problem is

$$\begin{aligned} \langle \mathcal{A}^{-1} \bar{d}^{-1} m(u), -\mathcal{A}^{-1} \frac{\delta \bar{d}}{\bar{d}^2} m(u) \rangle &= 0 \quad \forall \delta \bar{d}, \int \delta \bar{d} = 0 \\ \int \frac{m(u)}{\bar{d}^2} \delta \bar{d} \mathcal{A}^{-*} \mathcal{A}^{-1} \bar{d}^{-1} m(u) dx &= 0 \quad \forall \delta \bar{d}, \int \delta \bar{d} = 0 \end{aligned}$$

As $\int \delta \bar{d} = 0$, we deduce that

$$\frac{m(u)}{\bar{d}^2} \mathcal{A}^{-*} \mathcal{A}^{-1} \bar{d}^{-1} m(u) = C$$

where C is independant of N .

Since $\mathcal{A}^{-*} \phi$, for any ϕ vanishes at boundary of Ω , the only possible value of C is zero. but the factor $\frac{m(u)}{\bar{d}^2}$ never vanishes, and so we get:

$$\mathcal{A}^{-*} \mathcal{A}^{-1} \bar{d}^{-1} m(u) = 0$$

which implies:

$$\bar{d}^{-1} m(u) = 0$$

but this is also a positive number and we get a contradiction.

The critical point arising in this computation is related to the fact that independently of the mesh size, the approximate solution is always exact on the boundary. The ideal mesh density should be zero on the boundary and much higher just in the vicinity of the boundary. In other words, optimality system has no smooth enough solution. In order to cure this point, we propose to introduce at the same time both solution smoothness and minimum problem compactness.

2.4 Regularized optimisation problem

In order to overcome the previous paradox, it is possible to regularize the problem in H^1 when a penalty term depending on the inverse of d is added. Indeed, for any strictly positive function d of $H^1(\Omega)$, we put:

$$J(d) = J_1(d) + J_2(d) + J_3(d^{-1})$$

with

$$\begin{aligned} J_1(d) &= |\mathcal{A}^{-1} d^{-1} m(u)|_{L^2}^2 \\ J_2(d) &= \varepsilon |d|_{H^1}^2 \quad \text{with} \quad |d|_{H^1}^2 = |d|_{L^2}^2 + |\nabla d|_{L^2}^2 \\ J_3(d^{-1}) &= \eta |d^{-1}|_{L^2}^2 \end{aligned}$$

to be minimized under the constraints:

$$\int d = N ,$$

Lemma 1: *The above problem has at least a solution.*

The proof of this lemma relies on functional optimisation techniques, which can be found in [5]. Let (d_n) a sequence minimizing J under the two above constraints:

$$J(d_n) \rightarrow \text{Inf} J \tag{4}$$

Since $J(d_n)$ is bounded, this sequence stays in a ball of H^1 , the sequence d_n^{-1} in a ball of L^2 , and we can extract a subsequence (still denoted (d_n)) that minimises J and converges weakly:

$$d_n \rightarrow d^* \text{ weakly in } H^1$$

which implies, from classical injection compactness (and further extractions of subsequences),

$$d_n \rightarrow d^* \text{ strongly in } L^2$$

$$d_n^{-1} \rightarrow k^* \text{ weakly in } L^2$$

For any smooth function ϕ ,

$$(\phi d_n, d_n^{-1}) = (\phi(d_n - d^*), d_n^{-1}) + (\phi d^*, d_n^{-1})$$

Using Cauchy-Schwarz inequality, we obtain that

$$(\phi(d_n - d^*), d_n^{-1}) \rightarrow 0$$

Using the weakly convergence of d_n^{-1} , we obtain that

$$(\phi d^*, d_n^{-1}) \rightarrow (\phi d^*, k^*)$$

We deduce that

$$(\phi d_n, d_n^{-1}) \rightarrow (\phi d^*, k^*).$$

But

$$(\phi d_n, d_n^{-1}) = \int \phi$$

and

$$(\phi d^*, k^*) = \int \phi d^* k^*$$

We conclude that $d^* k^* = 1$ a.e. i.e. $k^* = (d^*)^{-1}$ a.e..

It remains to pass to the limit in these lower semi-continuous functionals:

$$J_1(d^*) \leq \liminf J_1(d_n)$$

$$J_2(d^*) \leq \liminf J_2(d_n)$$

$$J_3((d^{-1})^*) \leq \liminf J_3((d_n)^{-1})$$

where the “lim” is taken for a n' tending to ∞ , and the “Inf” is taken for any n larger than n' . Then:

$$J_1(d^*) + J_2(d^*) + J_3((d^{-1})^*) \leq \liminf (J_1(d_n) + J_2(d_n) + J_3((d_n)^{-1})) = \inf J.$$

and d^* is an optimum. \square

2.5 Optimality conditions

The optimality conditions of the regularized problem is that for any δd such that $\int \delta d = 0$, we have:

$$\begin{aligned} < \mathcal{A}^{-1} d^{-1} m(u), -\mathcal{A}^{-1} \frac{\delta d}{d^2} m(u) >_{L^2} + \\ & \varepsilon < d, \delta d >_{L^2} + \varepsilon < \nabla d, \nabla \delta d >_{L^2} - \eta < d^{-1}, d^{-2} \delta d >_{L^2} = 0 \end{aligned}$$

or:

$$\int \frac{m(u)}{d^2} \delta d \mathcal{A}^{-*} \mathcal{A}^{-1} d^{-1} m(u) + \varepsilon < d, \delta d >_{L^2} + \varepsilon < \nabla d, \nabla \delta d >_{L^2} - \eta < d^{-1}, d^{-2} \delta d >_{L^2} = 0.$$

As $\int \delta d = 0$, we deduce (formally) that

$$- \varepsilon \Delta d + \varepsilon d + \frac{m(u)}{d^2} \mathcal{A}^{-*} \mathcal{A}^{-1} d^{-1} m(u) - \eta d^{-3} = C$$

where C is independant of N , and it appears also from the integration by parts a Neumann boundary condition (n outward unit normal to $\partial\Omega$):

$$\frac{\partial d}{\partial n} = 0 \text{ on } \partial\Omega. \quad (5)$$

We observe that both ε and η terms contribute to avoid the previous paradox.

3 A finite-element based continuous model

We concentrate on the usual Poisson problem in a polyhedral n -dimensional domain:

$$-\Delta u = f \text{ on } \Omega ; u = 0 \text{ on } \partial\Omega. \quad (6)$$

whose variational form writes:

$$a(u, v) = \int_{\Omega} \nabla u \cdot \nabla v \, dx = \langle f, v \rangle \quad \forall v \in V \quad (7)$$

where V holds for the Sobolev space $H_0^1(\Omega) = \{u \in L^2(\Omega), \nabla u \in (L^2(\Omega))^n, u|_{\partial\Omega} = 0\}$. Let \mathcal{T}_h be a mesh of Ω made of simplexes, let V_h be the subspace of V of continuous functions that are \mathcal{P}_1 on each element of the mesh. The discrete variational problem is

$$a(u_h, v_h) = \langle f, v_h \rangle \quad \forall v_h \in V_h \quad (8)$$

A posteriori error estimates have been derived by many authors for this approximation (see [2],[12]). These analyses propose different forms of the leading term of the error.

A priori estimates have been derived much more earlier, in $H^1(\Omega)$ (“projection property”), and in $L^2(\Omega)$ (Aubin-Nitsche analysis), but only by means of inequalities, and the leading term of the error is generally not exhibited (only bounds of it are proposed).

The approximation error in the sequel will be split into two components:

$$u_h - u = u_h - \Pi_h u + \Pi_h u - u. \quad (9)$$

We recognize in the first difference $\Pi_h u - u$ the *interpolation error*, and we shall refer to the second difference $u_h - \Pi_h u$ as the *implicit error*.

3.1 Implicit error

The implicit error is inside the discrete approximation space. Classically we can estimate it by writing that the finite-element solution is better than a direct projection of the continuous unknown. We try proceed with equalities. We assume for simplicity that the right-hand side f is exactly integrated. The discrete system writes:

$$a(u_h, v_h) = (f, v_h) \quad \forall v_h \in V_h \quad (10)$$

Let $\bar{\Pi}_h$ be a projection operator from V onto V_h . For any v in V its projection $\bar{\Pi}_h v$ is in V_h , thus

$$a(u_h, \bar{\Pi}_h v) = (f, \bar{\Pi}_h v) \quad \forall v \in V$$

then appears the continuous differential operator:

$$((-\Delta)u_h, \bar{\Pi}_h v) = (f, \bar{\Pi}_h v) \quad \forall v \in V \quad (11)$$

where the first product is the duality one between $H_0^1(\Omega)$ and $H^{-1}(\Omega)$. We also use the adjoint of the projector:

$$(\bar{\Pi}_h^*(-\Delta)u_h, v) = (\bar{\Pi}_h^* f, v) \quad \forall v \in V \quad (12)$$

Thus

$$\bar{\Pi}_h^*(-\Delta)u_h = \bar{\Pi}_h^* f \text{ in } V'$$

This allows the following error analysis:

$$\begin{aligned} \bar{\Pi}_h^*(-\Delta)u_h - \bar{\Pi}_h^*(-\Delta)\bar{\Pi}_h u &= \bar{\Pi}_h^* f - \bar{\Pi}_h^*(-\Delta)\bar{\Pi}_h u \text{ in } V' \\ \bar{\Pi}_h^*(-\Delta)(u_h - \bar{\Pi}_h u) &= \bar{\Pi}_h^*(-\Delta)(u - \bar{\Pi}_h u) \text{ in } V' \end{aligned} \quad (13)$$

where $\bar{\Pi}_h^*(-\Delta)$ can be inverted on adhoc spaces, or, equivalently in variational form:

$$\langle \nabla(u_h - \bar{\Pi}_h u), \nabla \bar{\Pi}_h \phi \rangle = \langle \nabla(u - \bar{\Pi}_h u), \nabla \bar{\Pi}_h \phi \rangle \quad (14)$$

For u and ϕ smooth, and by a density argument, the above calculation extends to the usual interpolation Π_h which will be considered in the sequel. This is an *a priori* analysis since we express the error $u_h - \Pi_h u$ as a function of the unknown u .

Orientation: To fix our vocabulary, we observe that we have identified three terms in our error analysis:

- the interpolation or projection error $u - \Pi_h u$, it is a *local error* in the sense that a local change in the mesh would produce only local a change in this error,
- its complement to global approximation error is the *implicit error*

$$E_h = u_h - \Pi_h u,$$

a nonlocal error. The implicit error is the solution of a (discrete) elliptic system with as right-hand side the truncation error,

$$\langle \nabla E_h, \nabla \Pi_h \phi \rangle = \langle \nabla(u - \Pi_h u), \nabla \Pi_h \phi \rangle \quad (15)$$

- the *truncation error* $\Pi_h^*(-\Delta)(u - \Pi_h u)$ is a local error that is, in the present case, expressed in terms of the interpolation error.

We now analyse the truncation error.

3.2 Truncation error analysis

In this paper we make the choice of a family of isotropic meshes in the sense that they have a quasi-uniform aspect ratio equal to unity. A mesh of this family is represented by a scalar local mesh size $\Delta x = \Delta y = m(x, y)$.

As announced in the introduction section of this paper, we are considering h -families of meshes for which the local step $m_h = h m$. Here the normalized function m of (x, y) does not depend on h .

An important consequence is that we automatically assume that for a fine enough mesh, the variation of mesh size between two neighboring cells can be made as small as we wish, as far as the normalized metric is smooth enough.

In an extremely regular mesh, the main part of error can show compensations between two neighboring elements. For a smooth function u , the approximate gradient $\nabla \Pi_h u$ can be of first order accuracy on a given equilateral triangle $T_1 = ABC, CA = CB$, while being (weakly) of second order accuracy on the union of this triangle with the triangle T_2 symmetric with respect to the basis AB (Fig.1).

Let us introduce, for a function ϕ in $C^3(\bar{\Omega})$, the following notation:

$$O_\phi(h^\alpha) \leq K h^\alpha \|\phi\|_{C^3(\bar{\Omega})}.$$

We shall denote $\mathcal{D}_3(\Omega)$ the subset of $C^3(\bar{\Omega})$ of functions with a compact support in Ω .

The following estimate is established in the Appendix:

Lemma 2: We assume that the continuous solution u is in $C^3(\bar{\Omega})$ and that the continuous mesh size m is in $C^0(\bar{\Omega})$. Then, for any function ϕ of $\mathcal{D}_3(\Omega)$, we have

$$\int_{\Omega} \frac{\partial(u - \Pi_h u)}{\partial x} \frac{\partial \Pi_h \phi}{\partial x} dM + \int_{\Omega} \frac{\partial(u - \Pi_h u)}{\partial y} \frac{\partial \Pi_h \phi}{\partial y} dM = h^2 (g(m), \phi) + O_\phi(h^3) \quad (16)$$

with $g(m) = g_1(m) + g_2(m)$:

$$\begin{aligned} (g_1(m), \phi) &= \frac{3}{48} \int_{\Omega} m^2 \frac{\partial^3 u}{\partial x \partial y^2} \frac{\partial \phi}{\partial x} dM - \frac{1}{48} \int_{\Omega} m^2 \frac{\partial^3 u}{\partial x^3} \frac{\partial \phi}{\partial x} dM \\ (g_2(m), \phi) &= \frac{1}{4} \int_{\Omega} \frac{m^2}{6} \frac{\partial \phi}{\partial y} \frac{\partial^3 u}{\partial x^2 \partial y} + m^2 \frac{\partial^2 \phi}{\partial y^2} \frac{\partial^2 u}{\partial x^2} dM \\ &\quad - \frac{3}{24} \int_{\Omega} m^2 \frac{\partial \phi}{\partial y} \frac{\partial^3 u}{\partial y^3} + m^2 \frac{\partial^2 \phi}{\partial y^2} \frac{\partial^2 u}{\partial y^2} dM \quad .\square \end{aligned}$$

In fact, for a smooth m , the distribution g is also smooth, by the magic of integration by parts:

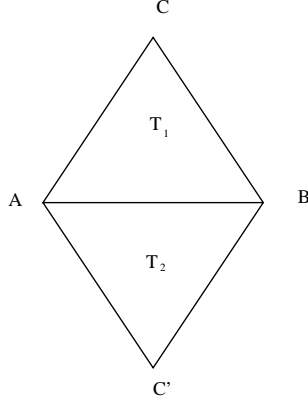


Figure 1: Error analysis on a regular mesh

Lemma 3: We assume that the continuous solution u is in $C^3(\bar{\Omega})$ and that the continuous mesh size m is in $C^2(\bar{\Omega})$. Then, for any function ϕ of $\mathcal{D}_3(\Omega)$, we have

$$\int_{\Omega} \frac{\partial(u - \Pi_h u)}{\partial x} \frac{\partial \Pi_h \phi}{\partial x} dM + \int_{\Omega} \frac{\partial(u - \Pi_h u)}{\partial y} \frac{\partial \Pi_h \phi}{\partial y} dM = h^2 (g'(m), \phi) + O_{\phi}(h^3) \quad (17)$$

with $g'(m) = g'_1(m) + g'_2(m)$:

$$(g'_1(m), \phi) = -\frac{3}{48} \int_{\Omega} \phi \frac{\partial}{\partial y} \left(m^2 \frac{\partial^3 u}{\partial x \partial y^2} \right) dM + \frac{1}{48} \int_{\Omega} \phi \frac{\partial}{\partial x} \left(m^2 \frac{\partial^3 u}{\partial x^3} \right) dM$$

$$\begin{aligned} (g'_2(m), \phi) &= -\frac{1}{4} \int_{\Omega} \phi \frac{\partial}{\partial y} \left(\frac{m^2}{6} \frac{\partial^3 u}{\partial x^2 \partial y} \right) + \phi \frac{\partial^2}{\partial y^2} \left(m^2 \frac{\partial^2 u}{\partial x^2} \right) dM \\ &\quad + \frac{3}{24} \int_{\Omega} \phi \frac{\partial}{\partial y} \left(m^2 \frac{\partial^3 u}{\partial y^3} \right) + \phi \frac{\partial^2}{\partial y^2} \left(m^2 \frac{\partial^2 u}{\partial y^2} \right) dM \quad \square \end{aligned}$$

3.3 Implicit error model

The above Lemma 2 states that, for any function of $\mathcal{D}_3(\Omega)$,

$$(\nabla E_h, \nabla \Pi_h \phi) = h^2 (g(m), \phi) + O_{\phi}(h^3) \quad (18)$$

where the first term of right hand side involves the application of a distribution $g(m)$ on a function ϕ of $\mathcal{D}_3(\Omega)$. Further, the above formula shows that for smooth (C^{∞}) u and m , the

distribution $g(m)$ is also smooth. Let us define:

$$\bar{E}_h = h^{-2} E_h . \quad (19)$$

Let us consider now the solution \tilde{E}_m of the continuous system

$$\tilde{E}_m \in H_0^1(\Omega), \text{ and } \left(\nabla \tilde{E}_m, \nabla \phi \right) = (g'(m), \phi) \quad \forall \phi \in H_0^1(\Omega) . \quad (20)$$

Since $g(m)$ is smooth. So is \tilde{E}_m .

Lemma 4: We have:

$$\left(\nabla E_h, \nabla(\Pi_h \phi) \right) = h^2 \left(\nabla \tilde{E}_m, \nabla(\Pi_h \phi) \right) + O_\phi(h^3) , \quad (21)$$

$$\left(\nabla E_h, \nabla(\Pi_h \phi) \right) = h^2 \left(\nabla \Pi_h \tilde{E}_m, \nabla(\Pi_h \phi) \right) + O_\phi(h^3) . \quad (22)$$

Proof: It is enough to estimate the difference:

$$G_h = \bar{E}_h - \Pi_h \tilde{E}_m \quad (23)$$

since \tilde{E}_m is smooth, which implies:

$$\begin{aligned} \left(\nabla G_h, \nabla(\Pi_h \phi) \right) &= \left(\nabla(\bar{E}_h - \tilde{E}_m), \nabla(\Pi_h \phi) \right) \\ &= - \left(\nabla(\Pi_h \tilde{E}_m - \tilde{E}_m), \nabla(\Pi_h \phi) \right) \\ &= O_\phi(h) . \end{aligned} \quad (24)$$

from the other side, we have

$$\left(\nabla G_h, \nabla(\Pi_h \phi) \right) = \left(\nabla \bar{E}_h, \nabla \Pi_h \phi \right) - \quad (25)$$

$$\left(\nabla(\Pi_h \tilde{E}_m - \tilde{E}_m), \nabla \Pi_h \phi \right) - \quad (26)$$

$$\left(\nabla \tilde{E}_m, \nabla(\Pi_h \phi - \phi) \right) - \quad (27)$$

$$\left(\nabla \tilde{E}_m, \nabla \phi \right) . \quad (28)$$

we observe that for a ϕ in $\mathcal{D}(\Omega)$ bounded in $\mathcal{C}^2(\bar{\Omega})$:

- due to \tilde{E}_m 's smoothness, term (27) is $O_\phi(h)$,
- since ϕ is bounded in $\mathcal{C}^1(\bar{\Omega})$ and \tilde{E}_m is smooth, term (26) is $O_\phi(h)$,
- due to (19) and (20), leading terms in (25) and (28) compensate. \square

Orientation : We have shown that:

$$\left(\nabla(\bar{E}_h - \Pi_h \tilde{E}_m), \nabla(\Pi_h \phi) \right) = O_\phi(h) .$$

We want now convince the reader that this result opens the door to a kind of *asymptotic expansion of approximate solution with respect to the mesh size*. Indeed, for a fixed ϕ , we have:

$$\begin{aligned} \int_{\Omega} \nabla u_h \nabla \Pi_h \phi dM - \int_{\Omega} \nabla u \nabla \phi dM &= (\nabla(\Pi_h u + u_h - \Pi_h u), \nabla \Pi_h \phi) - (\nabla u, \nabla \phi) \\ &= (\nabla(\Pi_h u - u), \nabla \phi) + \\ &\quad (\nabla \Pi_h u, \nabla(\Pi_h \phi - \phi)) + \\ &\quad h^2 \left(\nabla \Pi_h \tilde{E}_m, \nabla \Pi_h \phi \right) + O_\phi(h^3) . \end{aligned}$$

The last line of right-hand side involves the nonlocal terms while the two lines before are local interpolation errors. These local errors can be developed by the same techniques as in Appendix into the sum of purely continuous terms weighted by a factor h^2 plus $O_\phi(h^3)$ rests.

This is also the case for the last line, since:

$$\begin{aligned} h^2 \left(\nabla \Pi_h \tilde{E}_m, \nabla \Pi_h \phi \right) &= \\ &h^2 \left(\nabla \tilde{E}_m, \nabla \phi \right) + \\ &h^2 \left(\nabla(\Pi_h \tilde{E}_m - \tilde{E}_m), \nabla \Pi_h \phi \right) + \\ &h^2 \left(\nabla \tilde{E}_m, \nabla(\Pi_h \phi - \phi) \right) . \end{aligned}$$

and, due to the smoothness of \tilde{E}_m and ϕ , the two last terms are also $O_\phi(h^3)$.

As a conclusion we have shown that:

$$\int_{\Omega} \nabla u_h \nabla \Pi_h \phi dM = \int_{\Omega} \nabla u \nabla \phi dM + h^2 \int_{\Omega} \nabla \tilde{E}_m \nabla \phi dM + h^2 (g''(m, u), \phi) + O_\phi(h^3) .$$

where g'' a non-discrete smooth term involving \tilde{E}_m implicit terms and local terms. To deal with a strictly general case, an extra term should be added in order to take into account numerical integrations, in particular that of the right-hand side f of our model. For simplicity, we shall take now \tilde{E}_m as a model for the implicit error.

4 Optimal Control model

Given a metric $m(x, y)$ of the above family, we can define a continuous implicit error model as follows:

$$Y(m) \in H_0^1(\Omega) , \text{ and } \forall \phi \in H_0^1(\Omega) ,$$

$$\int_{\Omega} \nabla Y(m) \cdot \nabla \phi \, dM = \int_{\Omega} g'(m) \phi \, dM .$$

This Dirichlet problem can be interpreted as follows:

$$-\Delta Y(m) = g'(m)$$

$$Y(m) = 0 \text{ on } \partial\Omega$$

Now we are able to look for the best mesh for minimizing a given error. This is formulated as an Optimal Control problem. The control is the metric, the state variable is the solution $Y(\mathcal{M})$ of the above system and represents the approximation error.

Let J be a functional depending on both control and state and let us define:

$$j(m) = J(m, Y(m)) ,$$

the optimisation problem to solve writes:

$$\text{Find } m_{opt} = \text{ArgMin } j(m) .$$

New efficient algorithms are being developed in the litterature for solving Optimal Control problems with PDE's (let us refer to two recent contributions of ours [8],[6]).

5 Numerical experiments

The two above minimisation formulations define continuous optimal metrics. They cannot be solved but can be approximated by discrete problems. This can be done on an initial mesh. But *in fine* an accurate metric and mesh adaptation cannot be obtained without an external loop applying an adaptive mesh regeneration.

5.1 Adaptative mesh algorithm

In this paper, we restrict our optimisation experiments to the simplified finite-difference model (1) of Sec.2. The optimal local mesh size coupled with the error equation is a system of PDE. An approximate solution of it can be obtained by applying a discretization of the two independant variables that are (a) the PDE solution and (b) the metrics. We get a discrete optimisation problem which is solved by a gradient method. A fixed integral of mesh density is imposed by projecting corrections of m on the space of functions with vanishing integral. The above method will give an approximation of the "optimal metrics", that then can be used for building a new better mesh, but the accuracy of this approximation is directly dependant of the initial mesh and can be very bad.

At convergence of the Optimisation, an approximation of the optimal density is obtained.

We then apply a mesh adaptation algorithm which will provide an adapted mesh for a prescribed number of nodes.

In our experiments, mesh regeneration is obtained by applying the software BAMG. See [4] for details.

5.2 Numerical experiments: Finite Differences

The PDE under investigation is set in a two-dimensional unit square denoted by Ω . We consider the particular function f_1 :

$$u(x, y) = f_1(x, y) = (x^2 - x)(y^2 - y).$$

For any scalar continuous mesh density field d belonging to $H^1(\Omega)$, we want to find the minimum of:

$$J(d) = J_1(d) + J_2(d) + J_3(d^{-1})$$

with

$$\begin{aligned} J_1(d) &= |\mathcal{A}^{-1} d^{-1} m(u)|_{L^2}^2 = |u^{(4)}|^2 |\mathcal{A}^{-1} d^{-1}|_{L^2}^2 = 8^2 |\mathcal{A}^{-1} d^{-1}|_{L^2}^2 \\ J_2(d) &= \varepsilon |d|_{H^1}^2 \\ J_3(d^{-1}) &= \eta |d^{-1}|_{L^2}^2 \end{aligned}$$

under the constraint:

$$\int d = N.$$

Optimality conditions write:

$$\begin{aligned} -\varepsilon \Delta d + \varepsilon d + \frac{m(u)}{d^2} \mathcal{A}^{-*} \mathcal{A}^{-1} d^{-1} m(u) - \eta d^{-3} &= C \\ -\varepsilon \Delta d + \varepsilon d + \frac{8^2}{d^2} \mathcal{A}^{-*} \mathcal{A}^{-1} d^{-1} - \eta d^{-3} &= C \end{aligned}$$

where C does not depend on the total number of nodes N , and where

$$\frac{\partial d}{\partial n} = 0. \tag{29}$$

A first computation shows that the proposed error model is a rather good representation of the exact one, see Fig.2 for a comparison of both (they are maximum on center of domain, zero on boundary). As proposed in the Finite-Difference section, the error term of the functional is a L^2 norm of the error model. Penalty and regularisation terms are weighted with unit coefficients. The mesh is a 70×70 cartesian one. Then we can run a minimisation with respect to the density, starting from a uniform density, which in the particular case of this function, provides a uniform truncation error. The initial condition is thus somewhat quasi optimal. However, the optimisation made the functional decrease of about 50%. The effect of this mesh improvement is seen through several vertical cuts:

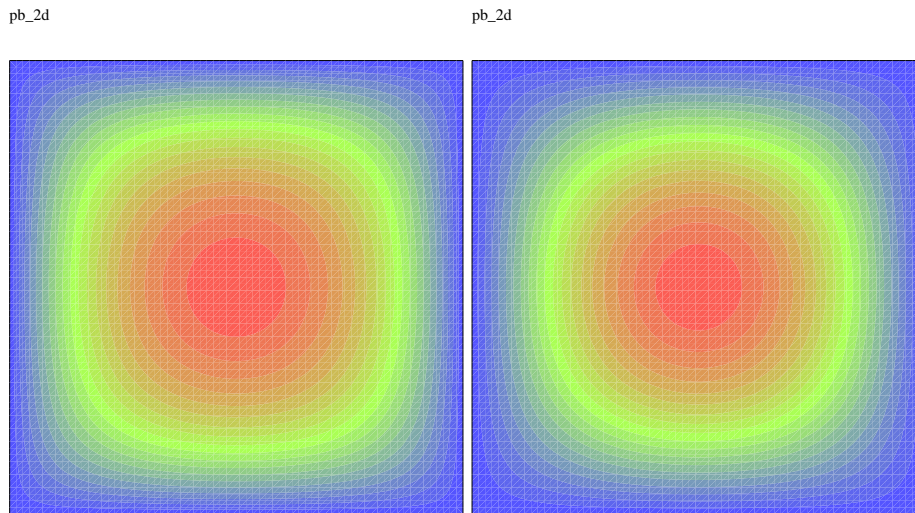


Figure 2: Comparison between the exact error and the proposed error model

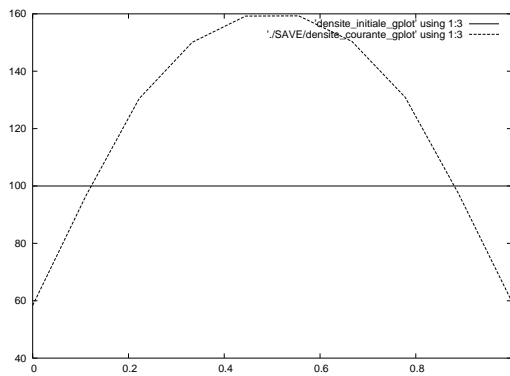


Figure 3: Finite Differences: initial and final mesh-densities

- the mesh density increases in the center, decreases at boundary, see Fig.3.
- the truncation error displayed in Fig.4, is reduced of 40% at the center of computational domain, and takes larger values at boundary,
- the approximation error model is reduced in any place of the computational domain, see Fig.5. A particular interest of the implicit error formulation is that we can try to minimise the approximation error on a subset of the computational domain. Now let us restrict the error integral to the half part on right of the domain. If we worked only with a local truncation model, then we would obtain an optimal mesh without nodes on the left part

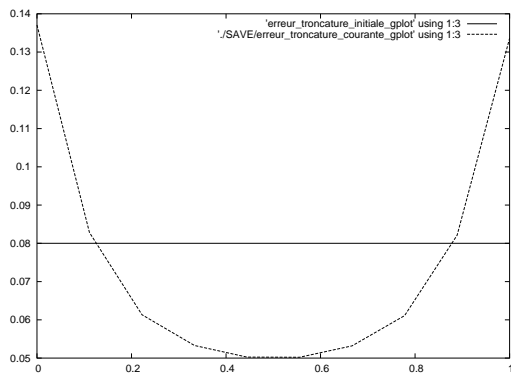


Figure 4: Finite Differences: initial and final truncation errors

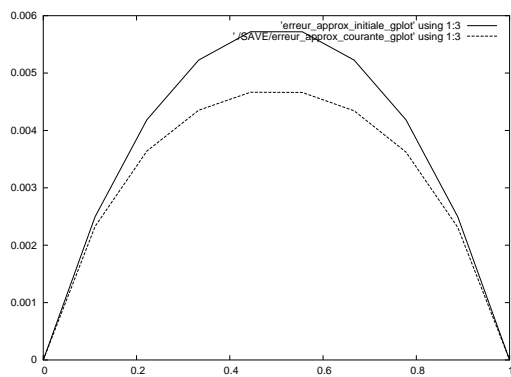


Figure 5: Finite Differences: initial and final approximation errors

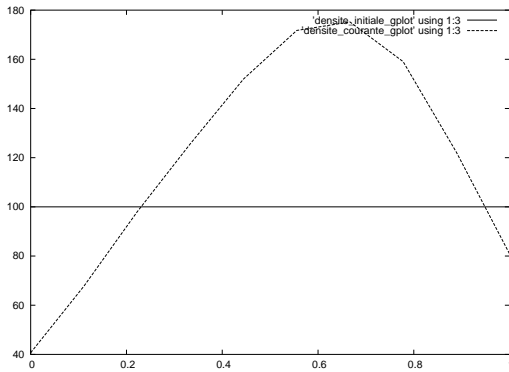


Figure 6: Finite Differences/right-sided observation: initial and final mesh-densities

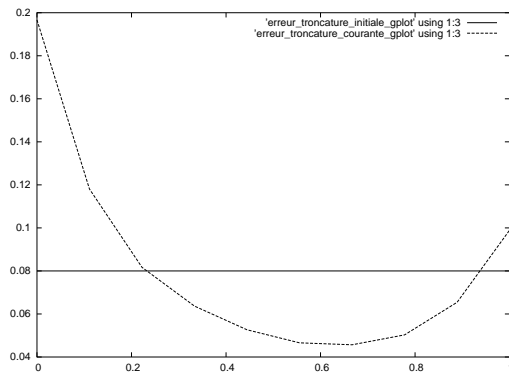


Figure 7: Finite Differences/right-sided observation: initial and final truncation errors

of the domain. Due to strong dependance of implicit errors over the mesh, the optimal mesh-density shows only a slight migration in the right direction, see Figs.6, 7,8.

6 Conclusions

We have explored two different aspects of optimal mesh continuous methods. The novelty is that the method is pushed to a complete optimal control theory, with a state system, a functional to minimize, an adjoint state for computing a functional gradient. If we choose an error norm over the whole domain as a functional, we show that this leads to introduce mesh-smoothness constraints or penalty terms. The error modelling for the simplest finite-element context demands to continue further *a priori* estimates.

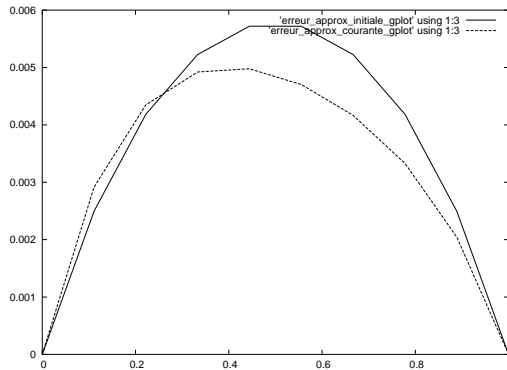


Figure 8: Finite Differences/right-sided observation: initial and final approximation errors

Some important potential advantages of the proposed methodology are listed now:

- As in *a posteriori* methods, the needs in accuracy can be specified by user under the form of a functional to compute accurately. This opens the door to a combination of adaptation with an optimal design loop.
- Further, the needs in accuracy can also be specified by user under the form of an error to minimize, as shown in the previous section.
- As in [7], the continuous model can be extended to the case where the solution presents some singularities. In that case error order is modelled and can be predicted as second-order for optimal meshes.

Before this, several difficulties have to be solved:

- An accurate enough approximation for the third or fourth derivatives of the unknown have to be introduced in order to treat a generic mesh adaptation problem.
- further analysis is needed in order to have a rigorous analysis of the relation between the model and discrete solutions. - as in Hessian-based methods, an ideal stretched mesh can then be modelled.

7 Appendix: Estimates for truncation term

This appendix deals with some estimates of the truncation term, and in particular with the proof of the following lemma:

Lemma 2:

$$\int_{\Omega} \frac{\partial(u - \Pi_h u)}{\partial x} \frac{\partial \Pi_h \phi}{\partial x} dM = \frac{(\Delta y)^2}{12} \int_{\Omega} \frac{\partial^3 u}{\partial x \partial y^2} \frac{\partial \phi}{\partial x} dM - \frac{(\Delta x)^2}{48} \int_{\Omega} \frac{\partial^3 u}{\partial x^3} \frac{\partial \phi}{\partial x} + o(h^2) \quad (30)$$

$$\int_{\Omega} \frac{\partial(u - \Pi_h u)}{\partial y} \frac{\partial \Pi_h \phi}{\partial y} dM = \frac{(\Delta x)^2}{4} \int_{\Omega} \frac{1}{6} \frac{\partial \phi}{\partial y} \frac{\partial^3 u}{\partial x^2 \partial y} + \frac{\partial^2 \phi}{\partial y^2} \frac{\partial^2 u}{\partial x^2} dM - \frac{(\Delta y)^2}{6} \int_{\Omega} \frac{\partial \phi}{\partial y} \frac{\partial^3 u}{\partial y^3} + \frac{\partial^2 \phi}{\partial y^2} \frac{\partial^2 u}{\partial y^2} dM + o(h^2) \quad (31)$$

7.1 Assumptions on mesh regularity

We consider a computational domain Ω which is partitioned in losanges:

$$L_{i,j} = (T_{i,j}^k)_{(i,j,k) \in [1..N] \times [1..P] \times [1,2]}$$

with centers:

$$A_{i,j} = \begin{pmatrix} x_i = a + i\Delta x \\ y_j = b + j\Delta y \end{pmatrix} \quad (32)$$

and $(a, b) \in R^2$. (cf. Fig. 9)

We denote by:

- H the projection of point $M \in L_{i,j}$ on $(A_{i,j}, A_{i+1,j})$ (cf. Fig 9)
- P the projection of point $M \in L_{i,j}$ on $(A_{i,j-1}, A_{i,j+1})$ (cf. Fig 10)
- $h = (\Delta x, \Delta y)$
- $P_{h,1} \subset H_0^1$ the subspace of continuous, linear-by-element functions $T_{i,j}^k$ which vanish on $\partial\Omega$
- u_h is the unique vector in H_0^1 which satisfies for any $v_h \in P_{h,1}$:

$$(\nabla u_h, \nabla v_h) = (f, v_h) \quad (33)$$

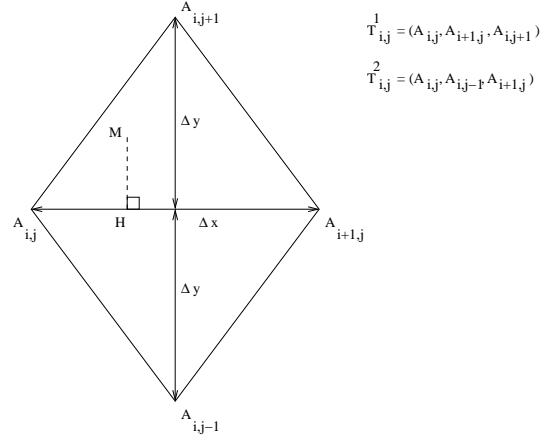


Figure 9: Regular pattern for the ideal mesh

- u is the unique vector in H_0^1 which satisfies for any $v \in H_0^1$

$$(\nabla u, \nabla v) = (f, v) \quad (34)$$

- $\Pi_h v$ is a mapping from a subspace \mathcal{V}_0 of H_0^1 to $P_{h,1}$ which will be the usual interpolation, in case of the considered functions are regular enough. but our results can be extended to Clement-type projections.

We are interested in the analysis of the truncation term:

$$T = (\nabla(u - \Pi_h u), \nabla \Pi_h \phi) \quad (35)$$

where ϕ is a test function of \mathcal{V}_0 . We split it into two terms:

$$T = A_1 + A_2 . \quad (36)$$

with :

$$A_1 = \int_{\Omega} \frac{\partial(u - \Pi_h u)}{\partial x} \frac{\partial \Pi_h \phi}{\partial x} dM , \quad (37)$$

and :

$$A_2 = \int_{\Omega} \frac{\partial(u - \Pi_h u)}{\partial y} \frac{\partial \Pi_h \phi}{\partial y} dM . \quad (38)$$

Another way to express this is:

$$(\nabla(u - \Pi_h u), \nabla \Pi_h \phi) = (\nabla(u - \Pi_h u), \nabla \phi) - (\nabla(u - \Pi_h u), \nabla(\phi - \Pi_h \phi)) \quad (39)$$

where we can make appear by integration by parts the interpolation error:

$$(\nabla(u - \Pi_h u), \nabla \phi) = (u - \Pi_h u, -\Delta \phi) . \quad (40)$$

Then it is also interesting to compute:

$$A'_1 = \int_{\Omega} \frac{\partial(u - \Pi_h u)}{\partial x} \frac{\partial(\phi - \Pi_h \phi)}{\partial x} dM , \quad (41)$$

$$A'_2 = \int_{\Omega} \frac{\partial(u - \Pi_h u)}{\partial y} \frac{\partial(\phi - \Pi_h \phi)}{\partial y} dM . \quad (42)$$

7.2 Study of A_1

Lemma 2a:

$$\int_{\Omega} \frac{\partial(u - \Pi_h u)}{\partial x} \frac{\partial \Pi_h \phi}{\partial x} dM = \frac{1}{12} \left(\int_{\Omega} \frac{\partial^3 u}{\partial x \partial y^2} \frac{\partial \phi}{\partial x} dM \right) (\Delta y)^2 - \frac{1}{48} \left(\int_{\Omega} \frac{\partial^3 u}{\partial x^3} \frac{\partial \phi}{\partial x} \right) (\Delta x)^2 + o(h^2) \quad (43)$$

.□

Proof: By translation, the computation of

$$\int_{L_{i,j}} \frac{\partial(u - \Pi_h u)}{\partial x} \frac{\partial \phi}{\partial x} dM$$

reduces to the computation of

$$\int_L \frac{\partial(u - \Pi_h u)}{\partial x} \frac{\partial \phi}{\partial x} dM .$$

Let us expand any integrand with respect to the distance to the center of losange, $O = (0, 0)$.

We get:

$$\frac{\partial u}{\partial x}(M) = \frac{\partial u}{\partial x}(O) + \nabla \left(\frac{\partial u}{\partial x} \right) (O) O\vec{M} + \frac{1}{2} O\vec{M} . H_{\frac{\partial u}{\partial x}}(O) . O\vec{M} + o(h^2) . \quad (44)$$

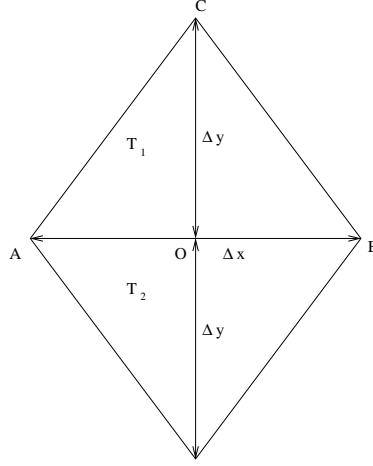


Figure 10: Simplified notations

From the other side,

$$\begin{aligned} \frac{\partial \Pi_h u}{\partial x}(M) &= \frac{u(B) - u(A)}{\Delta x} \\ u(B) &= u(O) + \frac{\Delta x}{2} \frac{\partial u}{\partial x}(O) + \frac{1}{2} \left(\frac{\Delta x}{2}\right)^2 \frac{\partial^2 u}{\partial x^2}(O) + \frac{1}{6} \left(\frac{\Delta x}{2}\right)^3 \frac{\partial^3 u}{\partial x^3}(O) + o((\Delta x)^2) \\ u(A) &= u(O) - \frac{\Delta x}{2} \frac{\partial u}{\partial x}(O) + \frac{1}{2} \left(\frac{\Delta x}{2}\right)^2 \frac{\partial^2 u}{\partial x^2}(O) - \frac{1}{6} \left(\frac{\Delta x}{2}\right)^3 \frac{\partial^3 u}{\partial x^3}(O) + o((\Delta x)^2) \end{aligned} \quad (45)$$

then

$$\frac{\partial \Pi_h u}{\partial x} = \frac{\partial u}{\partial x}(O) + \frac{1}{24} \frac{\partial^3 u}{\partial x^3}(O) (\Delta x)^2 + o(\|h\|^2) \quad (46)$$

and similarly for ϕ

$$\frac{\partial \Pi_h \phi}{\partial x} = \frac{\partial \phi}{\partial x}(O) + \frac{1}{24} \frac{\partial^3 \phi}{\partial x^3}(O) (\Delta x)^2 + o(\|h\|^2) . \quad (47)$$

We derive from Eqs. (44) and (46)

$$\frac{\partial(u - \Pi_h u)}{\partial x} = \nabla \left(\frac{\partial u}{\partial x} \right) (O) O\vec{M} + \frac{1}{2} O\vec{M} \cdot H_{\frac{\partial u}{\partial x}}(O) \cdot O\vec{M} - \frac{1}{24} \frac{\partial^3 u}{\partial x^3}(O) (\Delta x)^2 + o(\|h\|^2) \quad (48)$$

which, with (47) implies:

$$\begin{aligned}
 \int_L \frac{\partial(u - \Pi_h u)}{\partial x} \frac{\partial \Pi_h \phi}{\partial x} dM &= \frac{\partial \phi}{\partial x}(O) \nabla \left(\frac{\partial u}{\partial x} \right) (O) \int_L O \vec{M} dM \\
 &+ \frac{1}{2} \frac{\partial \phi}{\partial x}(O) \int_L O \vec{M} H_{\frac{\partial u}{\partial x}}(O) O \vec{M} dM \\
 &- \frac{1}{24} \frac{\partial^3 u}{\partial x^3}(O) \frac{\partial \phi}{\partial x}(O) (\Delta x)^2 \Delta x \Delta y + o(\Delta x \Delta y \|h\|^2)
 \end{aligned} \tag{49}$$

thus, by symmetry

$$\begin{aligned}
 \int_L \frac{\partial(u - \Pi_h u)}{\partial x} \frac{\partial \Pi_h \phi}{\partial x} dM &= \frac{1}{2} \frac{\partial \phi}{\partial x}(O) \int_L O \vec{M} H_{\frac{\partial u}{\partial x}}(O) O \vec{M} dM \\
 &- \frac{1}{24} \frac{\partial^3 u}{\partial x^3}(O) \frac{\partial \phi}{\partial x}(O) (\Delta x)^2 \Delta x \Delta y + o(\Delta x \Delta y \|h\|^2)
 \end{aligned} \tag{50}$$

now

$$\begin{aligned}
 \frac{1}{2} \frac{\partial \phi}{\partial x}(O) \int_L O \vec{M} H_{\frac{\partial u}{\partial x}}(O) O \vec{M} dM &= \frac{1}{2} \frac{\partial \phi}{\partial x}(O) \frac{\partial^3 u}{\partial x^3}(O) \int_L x^2 dM + \frac{\partial \phi}{\partial x}(O) \frac{\partial^3 u}{\partial x^2 \partial y} \int_L xy dM \\
 &+ \frac{1}{2} \frac{\partial^3 u}{\partial y^3}(O) \frac{\partial \phi}{\partial x}(O) \int_L y^2 dM
 \end{aligned} \tag{51}$$

then , since

$$\int_L x^2 dM = \frac{(\Delta x)^3 \Delta y}{24}$$

and,

$$\int_L xy dM = 0 \quad , \quad \int_L y^2 dM = \frac{(\Delta y)^3 \Delta x}{6}$$

we derive

$$\begin{aligned}
 \int_L \frac{\partial(u - \Pi_h u)}{\partial x} \frac{\partial \Pi_h \phi}{\partial x} dM &= \frac{\Delta x (\Delta y)^3}{12} \frac{\partial^3 u}{\partial x \partial y^2}(O) \frac{\partial \phi}{\partial x}(O) - \frac{\Delta y (\Delta x)^3}{48} \frac{\partial^3 u}{\partial x^3}(O) \frac{\partial \phi}{\partial x}(O) \\
 &+ o(\Delta x \Delta y \|h\|^2)
 \end{aligned} \tag{52}$$

and then finally:

$$\boxed{
 \begin{aligned}
 \int_{\Omega} \frac{\partial(u - \Pi_h u)}{\partial x} \frac{\partial \Pi_h \phi}{\partial x} dM &= \frac{1}{12} \left(\int_{\Omega} \frac{\partial^3 u}{\partial x \partial y^2} \frac{\partial \phi}{\partial x} dM \right) (\Delta y)^2 \\
 &- \frac{1}{48} \left(\int_{\Omega} \frac{\partial^3 u}{\partial x^3} \frac{\partial \phi}{\partial x} \right) (\Delta x)^2 + o(\|h\|^2)
 \end{aligned}
 } \tag{53}$$

7.3 Analysis of term A_2

Lemma 2b:

$$\int_{\Omega} \frac{\partial(u - \Pi_h u)}{\partial y} \frac{\partial \Pi_h \phi}{\partial y} dM = \frac{(\Delta x)^2}{4} \int_{\Omega} \frac{1}{6} \frac{\partial \phi}{\partial y} \frac{\partial^3 u}{\partial x^2 \partial y} + \frac{\partial^2 \phi}{\partial y^2} \frac{\partial^2 u}{\partial x^2} dM \quad (54)$$

$$- \frac{(\Delta y)^2}{6} \int_{\Omega} \frac{\partial \phi}{\partial y} \frac{\partial^3 u}{\partial y^3} + \frac{\partial^2 \phi}{\partial y^2} \frac{\partial^2 u}{\partial y^2} dM + o(\|h\|^2) \quad (55)$$

Proof: by translation, the evaluation of

$$\int_{L_{i,j}} \frac{\partial(u - \Pi_h u)}{\partial y} \frac{\partial \phi}{\partial y} dM$$

reduces to the one of

$$\int_L \frac{\partial(u - \Pi_h u)}{\partial y} \frac{\partial \phi}{\partial y} dM$$

we shall assume there exists $C \geq 0$ such that for any $M \in \Omega$ and for any $n \in N$, we have

$$\left| \frac{\partial^n u}{\partial y^n}(M) \right| \leq C. \quad (56)$$

We have also

$$\begin{aligned} \left(\frac{\partial \Pi_h u}{\partial y} \right)_{T_1} &= \frac{u(C) - u(O)}{\Delta y} \\ &= \frac{u(C) - \frac{u(A) + u(B)}{2}}{\Delta y} \end{aligned} \quad (57)$$

But:

$$u(A) = u(O) + \sum_{n=1}^{+\infty} \frac{1}{n!} \left(\frac{\Delta x}{2} \right)^n \frac{\partial^n u}{\partial x^n}(O) \quad (58)$$

and

$$u(B) = u(O) + \sum_{n=1}^{+\infty} \frac{1}{n!} \left(\frac{-\Delta x}{2} \right)^n \frac{\partial^n u}{\partial x^n}(O) \quad (59)$$

thus

$$\frac{u(A) + u(B)}{2} = u(O) + \sum_{p=1}^{+\infty} \left(\frac{\Delta x}{2} \right)^{2p} \frac{\partial^{2p} u}{\partial x^{2p}}(O) \quad (60)$$

and then

$$\left(\frac{\partial \Pi_h u}{\partial y}\right)_{T_1} = \frac{u(C) - u(O)}{\Delta y} - \frac{1}{\Delta y} \sum_{p=1}^{+\infty} \left(\frac{\Delta x}{2}\right)^{2p} \frac{\partial^{2p} u}{\partial x^{2p}}(O). \quad (61)$$

Therefore, since

$$\frac{u(C) - u(O)}{\Delta y} = \frac{\partial u}{\partial y}(O) + \frac{1}{2} \frac{\partial^2 u}{\partial y^2}(O)(\Delta y) + \frac{1}{6} \frac{\partial^3 u}{\partial y^3}(O)(\Delta y)^2 + o((\Delta y)^2) \quad (62)$$

we can deduce:

$$\left(\frac{\partial \Pi_h u}{\partial y}\right)_{T_1} = \frac{\partial u}{\partial y}(O) + \frac{1}{2} \frac{\partial^2 u}{\partial y^2}(O)(\Delta y) + \frac{1}{6} \frac{\partial^3 u}{\partial y^3}(O)(\Delta y)^2 - \frac{1}{\Delta y} \sum_{p=1}^{+\infty} \left(\frac{\Delta x}{2}\right)^{2p} \frac{\partial^{2p} u}{\partial x^{2p}}(O). \quad (63)$$

From the other side,

$$\left(\frac{\partial u}{\partial y}\right)_{T_1}(M) = \frac{\partial u}{\partial y}(O) + \nabla \left(\frac{\partial u}{\partial y}\right)(O) O\vec{M} + \frac{1}{2} O\vec{M} \cdot H_{\frac{\partial u}{\partial y}}(O) \cdot O\vec{M} + o(\|h\|^2). \quad (64)$$

Then

$$\begin{aligned} \left(\frac{\partial(u - \Pi_h u)}{\partial y}\right)_{T_1}(M) &= \left(\nabla \left(\frac{\partial u}{\partial y}\right)(O) O\vec{M} - \frac{1}{2} \frac{\partial^2 u}{\partial y^2}(O)(\Delta y)\right) + \frac{1}{2} O\vec{M} \cdot H_{\frac{\partial u}{\partial y}}(O) \cdot O\vec{M} \\ &\quad - \frac{1}{6} \frac{\partial^3 u}{\partial y^3}(O)(\Delta y)^2 + \frac{1}{\Delta y} \sum_{p=1}^{+\infty} \left(\frac{\Delta x}{2}\right)^{2p} \frac{\partial^{2p} u}{\partial x^{2p}}(O) \\ &\quad + o(\|h\|^2). \end{aligned} \quad (65)$$

Similarly:

$$\left(\frac{\partial \Pi_h u}{\partial y}\right)_{T_2} = \frac{\partial u}{\partial y}(O) - \frac{1}{2} \frac{\partial^2 u}{\partial y^2}(O)(\Delta y) + \frac{1}{6} \frac{\partial^3 u}{\partial y^3}(O)(\Delta y)^2 + \frac{1}{\Delta y} \sum_{p=1}^{+\infty} \left(\frac{\Delta x}{2}\right)^{2p} \frac{\partial^{2p} u}{\partial x^{2p}}(O) + o(\|h\|^2) \quad (66)$$

and

$$\begin{aligned} \left(\frac{\partial(u - \Pi_h u)}{\partial y}\right)_{T_2} &= \left(\nabla \left(\frac{\partial u}{\partial y}\right)(O) O\vec{M} + \frac{1}{2} \frac{\partial^2 u}{\partial y^2}(O)(\Delta y)\right) + \frac{1}{2} O\vec{M} \cdot H_{\frac{\partial u}{\partial y}}(O) \cdot O\vec{M} \\ &\quad - \frac{1}{6} \frac{\partial^3 u}{\partial y^3}(O)(\Delta y)^2 - \frac{1}{\Delta y} \sum_{p=1}^{+\infty} \left(\frac{\Delta x}{2}\right)^{2p} \frac{\partial^{2p} u}{\partial x^{2p}}(O) \\ &\quad + o(\|h\|^2). \end{aligned} \quad (67)$$

From Eq. (63), Eq. (65), Eq. (66) and Eq. (67) we get by symmetry:

$$\begin{aligned}
\int_L \frac{\partial(u - \Pi_h u)}{\partial y} \frac{\partial \Pi_h \phi}{\partial y} dM &= \frac{\partial \phi}{\partial y}(O) \int_{T_1} O \vec{M} \cdot H_{\frac{\partial u}{\partial y}}(O) \cdot O \vec{M} dM \\
&\quad - \frac{1}{3} \frac{\partial \phi}{\partial y}(O) \frac{\partial^3 u}{\partial y^3}(O) (\Delta y)^2 \frac{\Delta x \Delta y}{2} \\
&\quad + \frac{\partial^2 \phi}{\partial y^2}(O) \Delta y \int_{T_1} \nabla \left(\frac{\partial u}{\partial y} \right)(O) O \vec{M} dM \\
&\quad - \frac{1}{2} \frac{\partial^2 \phi}{\partial y^2} \frac{\partial^2 u}{\partial y^2}(O) (\Delta y)^2 \frac{\Delta x \Delta y}{2} \\
&\quad + \frac{\partial^2 \phi}{\partial y^2}(O) \left(\frac{\Delta x}{2} \right)^2 \frac{\partial^2 u}{\partial x^2}(O) \frac{\Delta x \Delta y}{2} + o(\Delta x \Delta y \|h\|^2).
\end{aligned} \tag{68}$$

Since

$$\begin{aligned}
\int_{T_1} x dM &= 0, \\
\int_{T_1} y dM &= 0 \\
\int_{T_1} x^2 dM &= \frac{(\Delta x)^3 \Delta y}{48} \\
\int_{T_1} xy dM &= 0
\end{aligned}$$

and

$$\begin{aligned}
\int_{T_1} y^2 dM &= \frac{(\Delta y)^3 \Delta x}{12} \\
\int_{T_1} O \vec{M} H_{\frac{\partial u}{\partial y}}(O) O \vec{M} dM &= \frac{\partial^3 u}{\partial x^2 \partial y}(O) \frac{(\Delta x)^3 \Delta y}{48} + \frac{\partial^3 u}{\partial y^3}(O) \frac{(\Delta y)^3 (\Delta x)}{12}
\end{aligned} \tag{69}$$

and

$$\int_{T_1} \nabla \left(\frac{\partial u}{\partial y} \right)(O) O \vec{M} dM = \frac{\partial^2 u}{\partial y^2}(O) \frac{(\Delta y)^2 \Delta x}{6} \tag{70}$$

we derive from Eq. (68), Eq. (69) et Eq. (70) that

$$\int_L \frac{\partial(u - \Pi_h u)}{\partial y} \frac{\partial \Pi_h \phi}{\partial y} dM = \left(\begin{array}{l} \frac{\partial \phi}{\partial y} \frac{\partial^3 u}{\partial x^2 \partial y}(O) \frac{(\Delta x)^2}{24} + \frac{1}{6} \frac{\partial \phi}{\partial y} \frac{\partial^3 u}{\partial y^3}(O) (\Delta y)^2 \\ - \frac{1}{3} \frac{\partial \phi}{\partial y} \frac{\partial^3 u}{\partial y^3}(O) (\Delta y)^2 + \frac{1}{3} \frac{\partial^2 \phi}{\partial y^2} \frac{\partial^2 u}{\partial y^2}(O) (\Delta y)^2 \\ - \frac{1}{2} \frac{\partial^2 \phi}{\partial y^2} \frac{\partial^2 u}{\partial y^2}(O) (\Delta y)^2 + \frac{1}{4} \frac{\partial^2 \phi}{\partial y^2} \frac{\partial^2 u}{\partial x^2}(O) (\Delta x)^2 \end{array} \right) \frac{\Delta x \Delta y}{2} + o(\Delta x \Delta y \|h\|^2). \tag{71}$$

Finally:

$$\int_{\Omega} \frac{\partial(u - \Pi_h u)}{\partial y} \frac{\partial \Pi_h \phi}{\partial y} dM = \frac{(\Delta x)^2}{4} \int_{\Omega} \frac{1}{6} \frac{\partial \phi}{\partial y} \frac{\partial^3 u}{\partial x^2 \partial y} + \frac{\partial^2 \phi}{\partial y^2} \frac{\partial^2 u}{\partial x^2} dM - \frac{(\Delta y)^2}{6} \int_{\Omega} \frac{\partial \phi}{\partial y} \frac{\partial^3 u}{\partial y^3} + \frac{\partial^2 \phi}{\partial y^2} \frac{\partial^2 u}{\partial y^2} dM + o(\|h\|^2) \quad (72)$$

7.4 Determination of main term of A'_1

We have state that:

$$\frac{\partial(u - \Pi_h u)}{\partial x} = \nabla \left(\frac{\partial u}{\partial x} \right) (O) O\vec{M} + \frac{1}{2} O\vec{M} \cdot H_{\frac{\partial u}{\partial x}}(O) \cdot O\vec{M} - \frac{1}{24} \frac{\partial^3 u}{\partial x^3} (O) (\Delta x)^2 + o(\|h\|^2) \quad (73)$$

and similarly':

$$\frac{\partial(\phi - \Pi_h \phi)}{\partial x} = \nabla \left(\frac{\partial \phi}{\partial x} \right) (O) O\vec{M} + \frac{1}{2} O\vec{M} \cdot H_{\frac{\partial \phi}{\partial x}}(O) \cdot O\vec{M} - \frac{1}{24} \frac{\partial^3 \phi}{\partial x^3} (O) (\Delta x)^2 + o(\|h\|^2). \quad (74)$$

Making the product and integreting over the losange, we get:

$$\int_L \frac{\partial(u - \Pi_h u)}{\partial x} \frac{\partial(\phi - \Pi_h \phi)}{\partial x} dM = \int_L (x^2 u_{xx} \phi_{xx} + xy(u_{xx} \phi_{xy} + u_{xy} \phi_{xx}) + y^2 u_{xy} \phi_{xy} + o(\|h\|^2)) dM, \quad (75)$$

where second derivatives are taken at point O . WE get then:

$$\int_L \frac{\partial(u - \Pi_h u)}{\partial x} \frac{\partial(\phi - \Pi_h \phi)}{\partial x} dM = \int_L (x^2 u_{xx} \phi_{xx} + xy(u_{xx} \phi_{xy} + u_{xy} \phi_{xx}) + y^2 u_{xy} \phi_{xy} + o(\|h\|^2)) dM, \quad (76)$$

that is:

$$\int_L \frac{\partial(u - \Pi_h u)}{\partial x} \frac{\partial(\phi - \Pi_h \phi)}{\partial x} dM = \frac{(\Delta x)^3 \Delta y}{24} \int_L u_{xx} \phi_{xx} dM + \frac{\Delta x (\Delta y)^3}{6} \int_L u_{xy} \phi_{xy} dM + \Delta x \Delta y o(\|h\|^2), \quad (77)$$

and finally:

$$\boxed{\int_{\Omega} \frac{\partial(u - \Pi_h u)}{\partial x} \frac{\partial(\phi - \Pi_h \phi)}{\partial x} dM = \frac{1}{24} \left(\int_{\Omega} \frac{\partial^2 u}{\partial x^2} \frac{\partial^2 \phi}{\partial x^2} dM \right) (\Delta x)^2 + \frac{1}{6} \left(\int_{\Omega} \frac{\partial^2 u}{\partial x \partial y} \frac{\partial^2 \phi}{\partial x \partial y} \right) (\Delta y)^2 + o(\|h\|^2)} \quad (78)$$

Remarque : This expansion is also useful for minimising the interpolation error in semi-norm H^1 :

$$\text{Min } \|\nabla(u - \Pi_h u)\|^2. \quad (79)$$

A similar analysis also holds for A'_2 .

References

- [1] F. Alauzet and B. Mohammadi. Optimisation 3D du nez d'un supersonique business jet basée sur l'adaptation de maillage. application à la réduction du bang sonique. Research report 5053, INRIA, 2003.
- [2] I. Babuska and T. Strouboulis. *The Finite Element Method and its reliability*. Oxford Scientific Publications, New York, 2001.
- [3] R. Becker and R. Rannacher. A feed-back approach to error control in finite element methods: basic analysis and examples. *East-West J. Numer. Math.*, 4:237–264, 1996.
- [4] M.J. Castro-Diaz, F. Hecht, B. Mohammadi, and P.-L. George. *Anisotropic adaptative mesh generation in two dimensions for CFD*, pages 181–192. Computational Fluids Dynamic '96, 1996.
- [5] J. Cea. *Optimisation : théorie et algorithmes*. Dunod, Paris, 1969.
- [6] F. Courty and A. Dervieux. *A SQP-like one-shot algorithm for optimal shape design*. Notes on Numerical Fluid Dynamics, V. Selmin Ed. , Springer, 2005. to appear.
- [7] F. Courty, D. Leservoisier, P.-L. George, and A. Dervieux. Continuous metrics and mesh optimization. *Applied Numerical Mathematics*, 2004. to appear.
- [8] A. Dervieux, F. Courty, T. Roy, M. Vázquez, and B. Koobus. Optimization loops for shape and error control: extended lecture notes. Research report 5413, INRIA, 2004.
- [9] W.G. Habashi, J. Dompierre, Y. Bourgault, D. Ait-Ali-Yahia, M. Fortin, and M.-G. Vallet. Anisotropic mesh adaptation: Towards user-independent, mesh-independent and solver-independent cfd solutions: Part I: General principles. *International Journal for Numerical Methods in Fluids*, 32:725–744, 2000.
- [10] E. Schall, D. Leservoisier, A. Dervieux, and B. Koobus. Mesh adaptation as a tool for certified computational aerodynamics. *International Journal for Numerical Methods in Fluids*, 45, 2004.
- [11] D.A. Venditi and D.L. Darmofal. Anisotropic grid adaptation for functional outputs: application to two-dimensional viscous flows. *J. Comput. Phys.*, 187:22–46, 2003.
- [12] R. Verfurth. A posteriori error estimates for nonlinear problems. finite element discretization of elliptic problems. *Math. of Comp.*, 62(206):445–475, 1994.



Unité de recherche INRIA Sophia Antipolis
2004, route des Lucioles - BP 93 - 06902 Sophia Antipolis Cedex (France)

Unité de recherche INRIA Futurs : Parc Club Orsay Université - ZAC des Vignes
4, rue Jacques Monod - 91893 ORSAY Cedex (France)

Unité de recherche INRIA Lorraine : LORIA, Technopôle de Nancy-Brabois - Campus scientifique
615, rue du Jardin Botanique - BP 101 - 54602 Villers-lès-Nancy Cedex (France)

Unité de recherche INRIA Rennes : IRISA, Campus universitaire de Beaulieu - 35042 Rennes Cedex (France)

Unité de recherche INRIA Rhône-Alpes : 655, avenue de l'Europe - 38334 Montbonnot Saint-Ismier (France)

Unité de recherche INRIA Rocquencourt : Domaine de Voluceau - Rocquencourt - BP 105 - 78153 Le Chesnay Cedex (France)

Éditeur
INRIA - Domaine de Voluceau - Rocquencourt, BP 105 - 78153 Le Chesnay Cedex (France)
<http://www.inria.fr>
ISSN 0249-6399